J Solid State Electrochem (1999) 3: 104–110 © Springer-Verlag 1999

ORIGINAL PAPER

Sung-Mo Moon · Su-Il Pyun

Effects of applied anodic potential and pH on the repassivation kinetics of pure aluminium in aqueous alkaline solution

Received: 1 April 1998 / Accepted: 3 July 1998

Abstract The repassivation kinetics of pure aluminium have been explored in aqueous alkaline solutions as functions of applied anodic potential and pH by using an abrading electrode technique and a rotating disc electrode. The repassivation rate of the abraded bare surface of pure aluminium increased with increasing applied anodic potential in aqueous alkaline solutions, while it decreased with increasing pH. These results revealed that the growth rate of the passivating oxide film is enhanced by an applied electric field, but it is lowered due to the chemical attack by hydroxyl ions. A potentiostatic anodic current decay transient obtained from the abraded electrode surface showed a constant repassivation rate in neutral and weakly alkaline solutions. In contrast, in concentrated alkaline solutions it was observed to consist of three stages: a high repassivation rate in the initial stage due to a high formation rate of the oxide film on the abraded bare surface; a zero value of the repassivation rate in the second stage due to the dissolution of the oxide film by the attack of OH^-; a high repassivation rate in the third stage due to a lowered dissolution rate of the oxide film. The dissolution rate of the passivating oxide film was observed to depend on the removal rate of aluminate ions from the oxide/solution interface.

Key words Abrading electrode technique · Aluminium · Oxide film · Potentiostatic current transient · Repassivation kinetics

Introduction

The corrosion and anodic polarisation behaviour of aluminium in alkaline solutions have been studied for the development of aluminium as an anode in metal/air batteries [1–10]. Several authors [5, 8] did not take into account the existence of a passivating oxide film on an open circuit in studying the mechanism of corrosion of pure aluminium and its alloys in aqueous alkaline solutions, while others [3, 9, 10] did consider the presence of the oxide film. In a previous paper [11], the presence of a passivating oxide film on pure aluminium at an open circuit was experimentally verified in alkaline solution by the increase in the open circuit potential obtained from the moment just after interrupting the abrading action on the specimen. Considering that the passivating oxide film acts as a barrier for charge transport, it is of great importance to study the repassivation kinetics of pure aluminium owing to the growth of the oxide film for better understanding the mechanism of corrosion of pure aluminium in alkaline solutions.

The repassivation kinetics of metals has been investigated by many authors [12–22] using an abrading electrode [14, 17, 19, 20], a scratching electrode [12, 19] and a breaking electrode [13, 17] in aqueous solutions. Pyun and Lee [20] reported that the repassivation kinetics of aluminium-silicon-copper alloy can be classified into three groups with chloride ion concentration in neutral solutions: (1) only repassivation related to the formation of the passivating oxide film at low concentrations of Cl^-; (2) competition between repassivation and film breakdown at intermediate concentrations of Cl^-; (3) only uniform metal dissolution at high concentrations of Cl^-. Kim and Pyun [18] investigated the effect of pH on the repassivation behaviour in acidic and neutral solutions containing Cl^-. However, little attention has been given to the repassivation kinetics of pure aluminium in alkaline solutions.

In the present work, the repassivation kinetics of pure aluminium have been explored in alkaline solutions as functions of the applied anodic potential and pH to complete the whole spectra of the repassivation kinetics of pure aluminium in aqueous solution. For this purpose, open-circuit potential transients, potentiostatic

S.-M. Moon · S.-I. Pyun (✉)
Department of Materials Science and Engineering,
Korea Advanced Institute of Science and Technology,
373-1 Kusong-Dong, Yusong-Gu, Daejon 305-701, Korea

current transients, potentiodynamic polarisation curves and a.c. impedance spectroscopy were obtained by using an abrading electrode and a rotating disc electrode in the alkaline solutions.

Experimental

In this work, two kinds of electrode specimens were made of 99.99% purity aluminum wire of diameter 1.2 mm and of 99.99% purity aluminum disc of diameter 4.46 mm. The wire and disc electrodes were set in a block of polyethylene and the upper surface of the block was ground with silicon carbide papers of 2000 grit to expose the cross section of the electrodes to the electrolytic solution.

The electrolytes used in this study were 0.5 M Na_2SO_4 solutions containing 0 M, 0.001 M, 0.01 M, 0.1 M and 1 M NaOH. In all the electrochemical experiments, a platinum gauze and a saturated calomel electrode (SCE) were used as the counter and reference electrodes, respectively.

An abrading electrode technique was employed to investigate the repassivation kinetics of pure aluminium in alkaline solutions, which was designed at this laboratory by Pyun and Hong [15]. The abrading action on the specimen allows the exposure of a bare aluminium surface to the solution by removing the surface oxide film mechanically. The characteristics of the apparatus and experimental procedures were detailed in previous papers [15, 20].

Open-circuit potential transients were recorded with time from the moment just after interrupting the abrading action on the pure aluminium wire specimen in the alkaline solutions. The values of the open-circuit potential on the bare and native oxide-covered surfaces were determined as a function of the pH of the solution.

Potentiodynamic polarisation experiments were conducted on the native oxide-covered pure aluminium static disc specimen by using a EG&G Model 273 Galvanostat/Potentiostat with a scan rate of 0.5 mV s^{-1} at the rotation rate of 0 rpm in alkaline solutions.

Potentiostatic current transients were obtained from the moment just after interrupting the abrading action on the pure aluminum wire specimen at various applied anodic potentials in the range from −1.3 V_{SCE} to 3 V_{SCE} in alkaline solutions. Potentiostatic current transients were also obtained from the moment just after applying an anodic potential of 0 V_{SCE} to the native oxide-covered pure aluminium rotating disc specimen at various rotation rates of the specimen in 0.5 M Na_2SO_4 + 0.1 M NaOH solution. The data acquisition period was 10^{-2} s, which was sufficient for the investigation of the repassivation kinetics of aluminium by the growth of an anodic oxide film. IR drops were minimised as only small areas of bare metal surface and low electrolyte resistance were provided.

A.c. impedance measurements were made on the native oxide-covered pure aluminium rotating disc specimen at an applied anodic potential of 0 V_{SCE} to elucidate the effect of rotation rate on the resistance of the oxide film on the specimen in 0.5 M Na_2SO_4 + 0.1 M NaOH solution. The measurements were performed with a Zahner IM5D impedance analyser by superimposing an a.c. signal of 5 mV amplitude on the d.c. potential over 0.1 to 10^5 Hz.

Results and discussion

Figure 1 presents open-circuit potential transients obtained from the moment just after interrupting the abrading action on the pure aluminium wire specimen in 0.5 M Na_2SO_4 (neutral) and 0.5 M Na_2SO_4 + 1 M NaOH (alkaline) solutions. Upon interrupting the abrading action, the open-circuit potential of pure aluminium increased with time and then reached the steady-state values of about −0.9 V_{SCE} and −1.55 V_{SCE} in the neutral and alkaline solutions, respectively. From Fig. 1 the difference in open-circuit potential between on the native oxide-covered surface and on the bare surface was determined to be about 0.68 V and 0.27 V in the neutral and alkaline solutions, respectively. Considering the fact that the abrading action allows the bare surface of the specimen to be exposed to the electrolytic solution, the increase in open circuit potential after interrupting the abrading action is caused by the formation and growth of a passivating oxide film on the bare surface of the pure aluminium, as suggested in the previous paper [11].

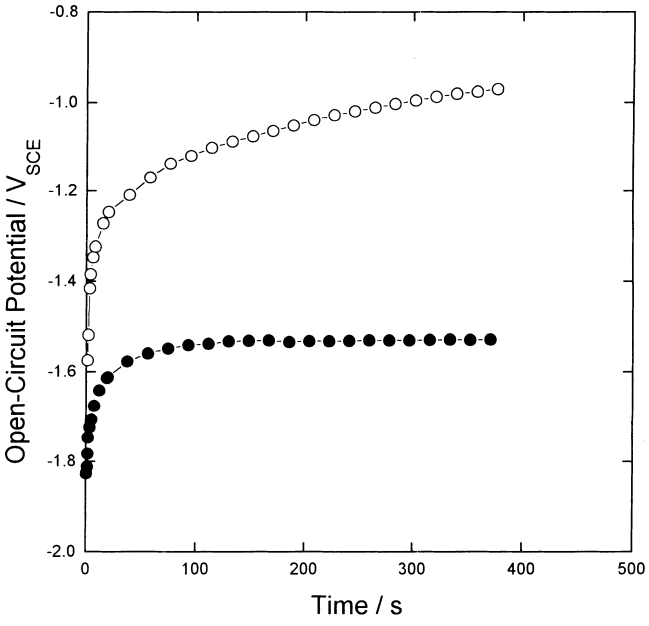

Fig. 1 Open-circuit potential transients obtained from the moment just after interrupting the abrading action on the pure aluminium wire specimen in 0.5 M Na_2SO_4 (○) (neutral) and 0.5 M Na_2SO_4 + 1 M NaOH (●) (alkaline) solutions

The open-circuit potential values obtained from the bare surface and from the native oxide-covered surface of pure aluminium are demonstrated in Fig. 2 as a function of the pH of the solution. The lines of ① and ② with the slopes of −0.059 and −0.079 V/pH represent equilibrium potentials of water reduction and aluminium dissolution reactions, respectively. It can readily be seen that the open-circuit potential values decreased with increasing pH with slopes of about −0.066 ± 0.002 and −0.056 ± 0.002 V/pH with increasing pH for the bare and native oxide-covered surfaces, respectively, lying always between the equilibrium potentials of water reduction and aluminium dissolution reactions. The values of these slopes ranged within the slopes of the equilibrium potentials of water reduction and aluminium dissolution reactions versus pH plots. This strongly indicated that the open circuit potentials of pure aluminium in alkaline solutions are just the mixed potentials which are determined from a combination of the

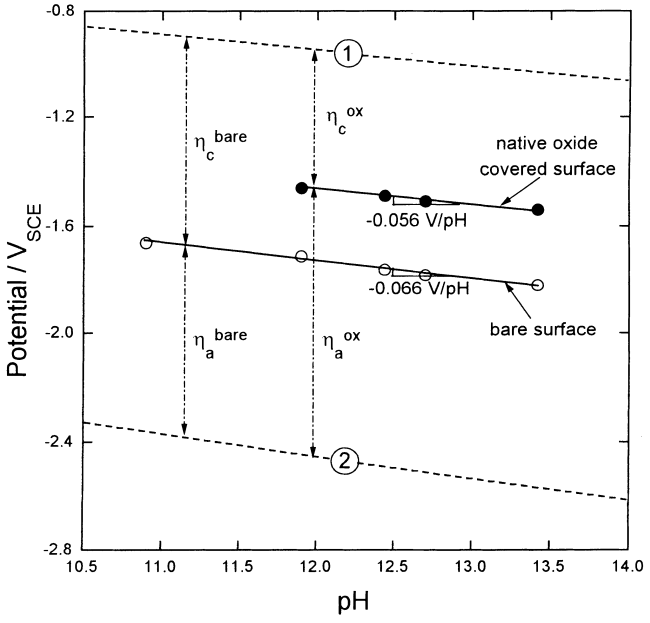

Fig. 2 Plots of open-circuit potential versus pH of the solution obtained from the bare surface (○) and from the oxide-covered surface (●) of a pure aluminium wire specimen in 0.5 M Na_2SO_4 solutions containing various concentrations of NaOH. η_a and η_c represent the amounts of anodic and cathodic polarisations, respectively

equilibrium potentials for water reduction and aluminium dissolution reactions.

The amount of anodic polarisation on the bare surface of pure aluminium on an open circuit, which is defined as the difference between the open circuit potential and the equilibrium potential of the aluminium dissolution reaction, was observed to be nearly the same as that of the cathodic polarisation, which is equal to be the difference between the equilibrium potential of the water reduction reaction and the open circuit potential. This reveals that the corrosion rate pure aluminium on the bare surface is controlled by both anodic and cathodic partial reactions. However, the amount of anodic polarisation on the native oxide-covered surface of pure aluminium appeared to be much larger than that of cathodic polarisation. In general, the cathodic or anodic polarisation will be present to a greater or lesser extent in most corrosion reactions. If one is more significant than the other, it will control the rate of the reaction. This leads to a classification of corrosion reactions according to whether the cathodic or anodic reaction is rate determining (cathodic control or anodic control). Thus, the larger amount of anodic polarisation means that corrosion of the native oxide-covered pure aluminium is anodically controlled.

Since the oxide film is spontaneously formed on the bare surface of pure aluminium (Fig. 1), the larger anodic polarisation is attributable to the presence of a passivating oxide film which significantly retards the rate of the anodic partial reaction. Thus, it is of great importance to examine the mechanism of formation and growth of the oxide film on the surface for a better understanding of the corrosion mechanism of pure aluminium in alkaline solution.

Figure 3 shows potentiodynamic polarisation curves of the native oxide-covered pure aluminium in 0.5 M Na_2SO_4 solutions containing various NaOH concentrations. As the concentration of sodium hydroxide increased, the passive current density increased and the corrosion potential shifted to more negative values. It is noted that the passive current density increased by about two orders as the concentration of sodium hydroxide increased from 0.001 M to 0.01 M compared to the increase by one order with increasing the concentration from 0.01 M to 0.1 M and 0.1 M to 1 M.

The anodic current density is plotted against time in Fig. 4 on a logarithmic scale obtained from the moment just after interrupting the abrading action on the pure aluminium wire specimen at various applied anodic potentials in 0.5 M Na_2SO_4 solution. The logarithmic current density linearly decreased with the logarithmic time. Considering that the charge and time involved are larger than those necessary for the double layer charging [20], it can be said that pure aluminium repassivates according to a log i–log t relationship [18, 20, 23] which can be written as

$$i = At^{-n} \tag{1}$$

where i is the anodic current density, A a constant, t the time and n represents the repassivation rate which is equal to the slope of the log i–log t plot.

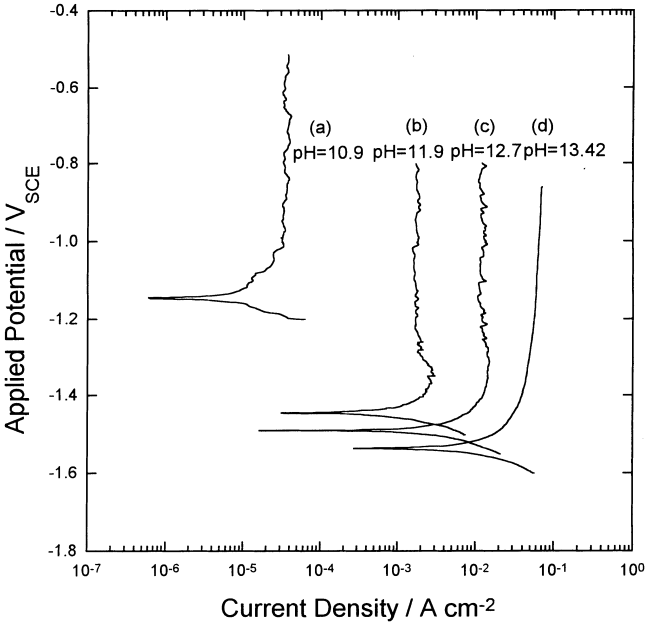

Fig. 3 Potentiodynamic polarisation curves of the pure aluminium static disc specimen with a scan rate of 0.5 mV s^{-1} at the rotation rate of 0 rpm in 0.5 M Na_2SO_4 solutions containing various NaOH concentrations of: *a* 0.001 M (pH = 10.90), *b* 0.01 M (pH = 11.90), *c* 0.1 M (pH = 12.70), *d* 1 M (pH = 13.42)

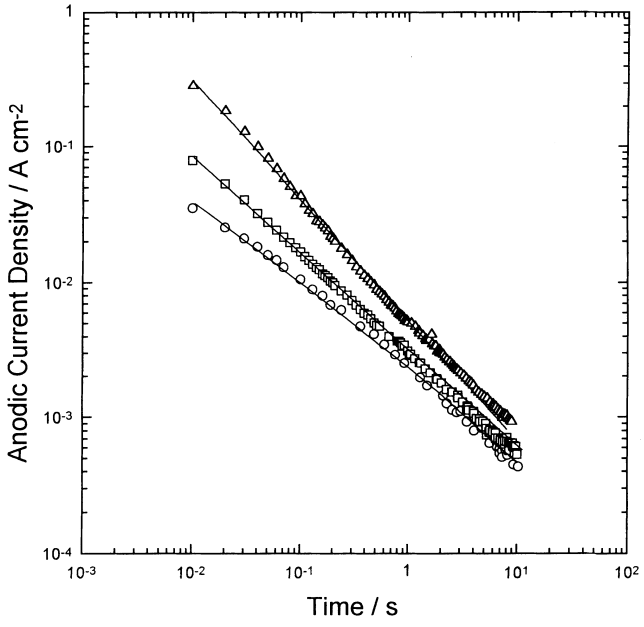

Fig. 4 Plots of anodic current density against time on a logarithmic scale obtained from the moment just after interrupting the abrading action on the pure aluminium wire specimen in 0.5 M Na_2SO_4 solution at various applied anodic potentials of: ○, −0.5 V_{SCE}; □, 0 V_{SCE}; △, 0.5 V_{SCE}

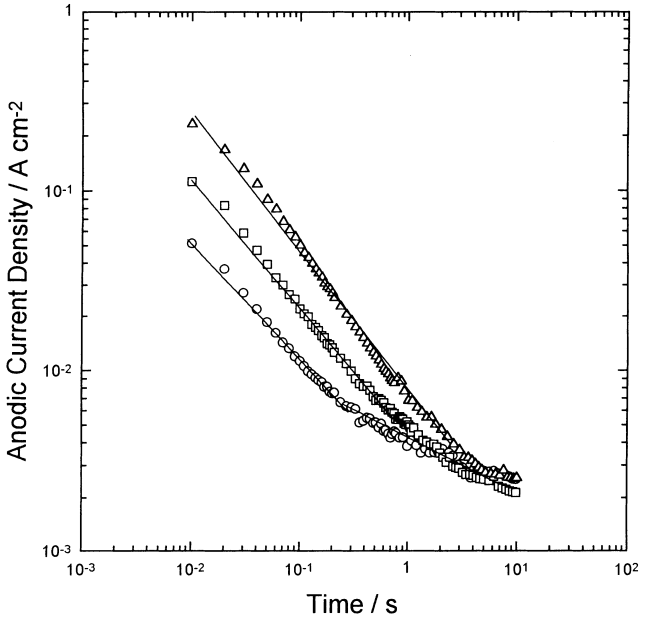

Fig. 6 Plots of anodic current density against time on a logarithmic scale obtained from the moment just after interrupting the abrading action on the pure aluminium wire specimen in 0.5 M Na_2SO_4 + 0.01 M NaOH solution at various applied anodic potentials of: ○, −1 V_{SCE}; □, 0 V_{SCE}; △, 1 V_{SCE}

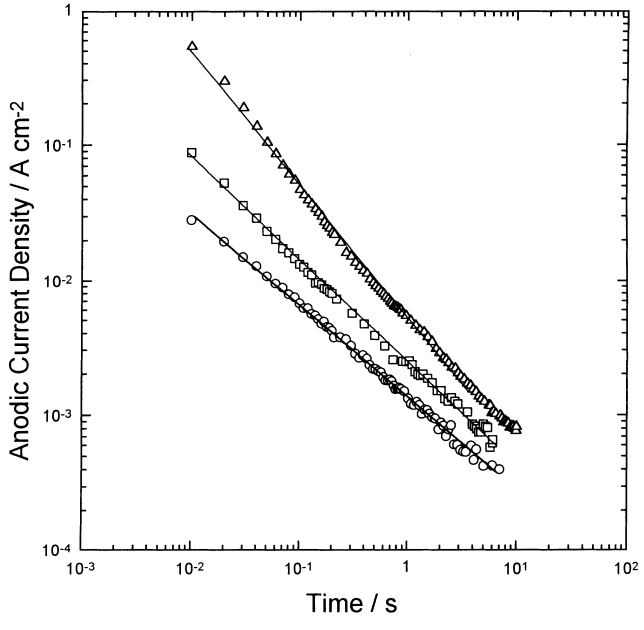

Fig. 5 Plots of anodic current density against time on a logarithmic scale obtained from the moment just after interrupting the abrading action on the pure aluminium wire specimen in 0.5 M Na_2SO_4 + 0.001 M NaOH solution at various applied anodic potentials of: ○, −0.5 V_{SCE}; □, 0 V_{SCE}; △, 0.5 V_{SCE}

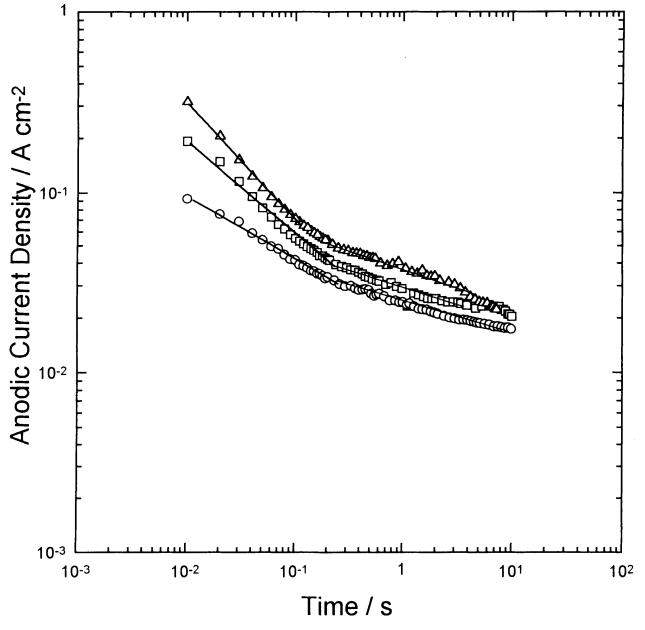

Fig. 7 Plots of anodic current density against time on a logarithmic scale obtained from the moment just after interrupting the abrading action on the pure aluminium wire specimen in 0.5 M Na_2SO_4 + 0.1 M NaOH solution at various applied anodic potentials of: ○, −1 V_{SCE}; □, 0 V_{SCE}; △, 1 V_{SCE}

Figures 5–8 give plots of the anodic current density against time on a logarithmic scale obtained from the moment just after interrupting the abrading action on the pure aluminium wire specimen at various applied anodic potentials in 0.5 M Na_2SO_4 solutions containing various NaOH concentrations of 0.001, 0.01, 0.1 and 1 M, respectively. In the presence of 0.001 M NaOH in 0.5 M Na_2SO_4 solution, the repassivation rate was observed to be a constant over the whole time (single-staged variation) as well as in the absence of NaOH in

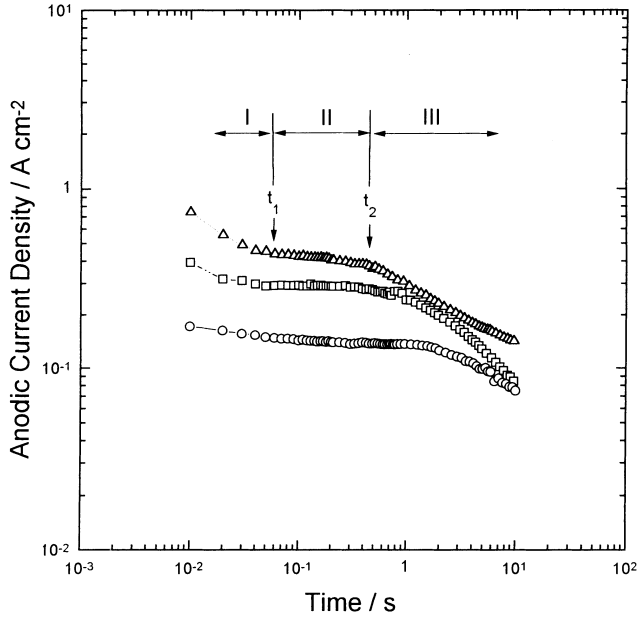

Fig. 8 Plots of anodic current density against time on a logarithmic scale obtained from the moment just after interrupting the abrading action on the pure aluminium wire specimen in 0.5 M Na_2SO_4 + 1 M NaOH solution at various applied anodic potentials of: ○, −1 V_{SCE}; □, 0 V_{SCE}; △, 1 V_{SCE}

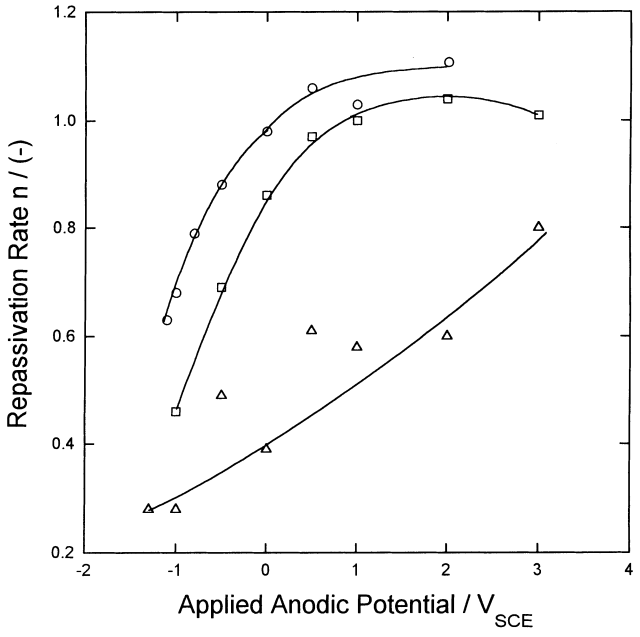

Fig. 9 Plots of repassivation rate of the pure aluminium wire specimen, n, against applied anodic potential in 0.5 M Na_2SO_4 solutions containing various NaOH concentrations of: ○, 0.001 M (pH = 10.90); □, 0.01 M (pH = 11.90); △, 0.1 M (pH = 12.70)

0.5 M Na_2SO_4 solution. However, in the presence of 0.01 M and 0.1 M NaOH in 0.5 M Na_2SO_4 solution, the repassivation rate showed a change from a higher value in the initial stage to a lower value in the later stage at around 0.2 s (two-staged variation). The lowered repassivation rate in the later stage is traced back to the attack by OH^- ions, which causes the dissolution of the oxide film according to

$$Al(OH)_3 + OH^- \longrightarrow Al(OH)_4^- \quad (2)$$

The repassivation rate in the initial stage of the repassivation is plotted in Fig. 9 against the applied anodic potential in 0.5 M Na_2SO_4 solutions containing various concentrations of NaOH. The repassivation rate increased with increasing applied anodic potential in alkaline solutions, while it showed much lower values with increasing hydroxide ion concentration at the same applied anodic potential. The increased repassivation rate with applied anodic potentials indicates the formation of a passivating oxide film on the surface which is enhanced by the applied electric field. By contrast, the decreased repassivation rate with hydroxide ion concentration means a lowered growth rate of passivating oxide film, which is assigned to chemical attack by hydroxide ions according to reaction (2).

Figure 10 depicts the plot of anodic current density against time on a logarithmic scale obtained from the moment just after interrupting the abrading action on the pure aluminium wire specimen at various applied anodic potentials in 1 M NaOH + 0.5 M Na_2SO_4 solution. The log i – log t plot appeared to be composed of three stages (three-staged variation). The first stage (I) corresponds to the descending current density up to t_1. The second stage (II) represents a constant current density region between t_1 and t_2. The third stage (III) corresponds to the decrease in current density after t_2. It is clear that the decrease of logarithmic current density in the first stage (I) is due to the fact that the formation rate of passivating oxide film dominates over its dissolution rate on the bare surface. The zero value of repassivation rate in the second stage (II) implies that the rate of oxide formation equals the rate of oxide dissolution so that the oxide film hardly grows.

However, if the oxide dissolution proceeds sufficiently, the dissolution rate of hydroxide film would be retarded by the enrichment of aluminate ions, $Al(OH)_4^-$, at the oxide/solution interface. This should cause the growth of the oxide film, thereby showing the high repassivation rate in the third stage (III) in Fig. 8. The concentration of $Al(OH)_4^-$ ions at the oxide/solution interface will be strongly dependent on the rate of their removal from the oxide/solution interface towards the bulk solution by diffusion.

In order to explore the effect of the concentration of hydroxide ions at the oxide/solution interface on the dissolution rate of the oxide film, the anodic current density was recorded with time at various rotation rates of the pure aluminium rotating disc specimen in 0.1 M NaOH + 0.5 M Na_2SO_4 solution, and the results are illustrated in Fig. 10. The anodic current density decreased with time and reached steady-state values at lower rotation rates of 0 and 50 rpm. At higher rotation rates above 100 rpm, it showed a minimum value and then reached steady-state values. The steady-state value

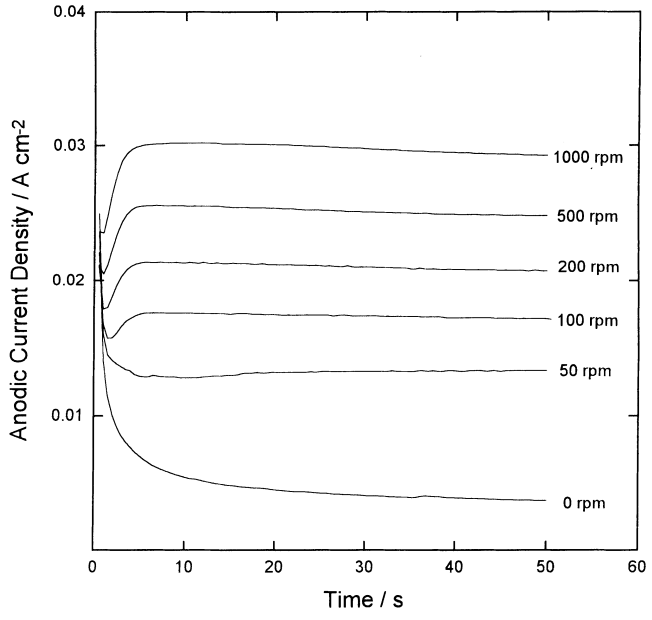

Fig. 10 Plots of anodic current density against time on a linear scale obtained from the moment just after applying an anodic potential of 1 V_{SCE} to the native oxide-covered pure aluminium rotating disc specimen at various rotation rates of the specimen in 0.5 M Na_2SO_4 + 1 M NaOH solution

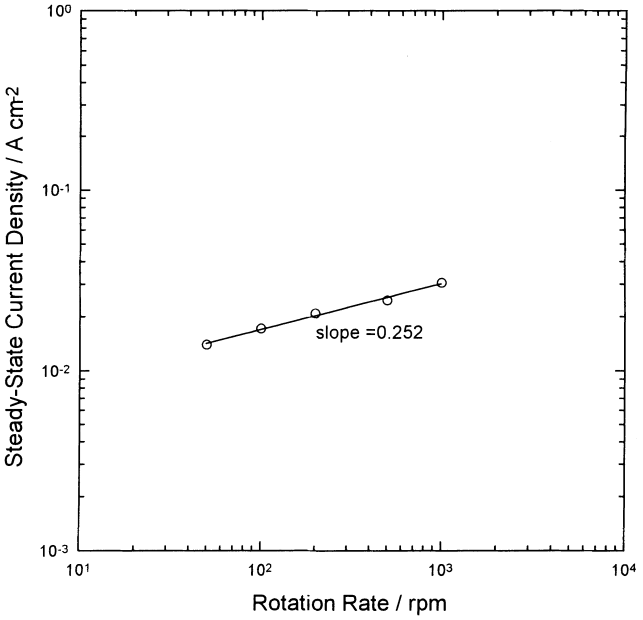

Fig. 11 Plot of steady-state anodic current density against rotation rate of the pure aluminium rotating disc specimen in 0.5 M Na_2SO_4 + 1 M NaOH solution obtained from Fig. 10

of the anodic current density increased with increasing rotation rate of the specimen.

Figure 11 shows the plot of the steady-state anodic current density against the rotation rate of the disc specimen on a logarithmic scale in 0.1 M NaOH + 0.5 M Na_2SO_4 solution. The slope of the plot of the steady-state anodic current density against the rotation rate was observed to be 0.252. This lower slope than 0.5 suggests that the anodic current density is not determined by the diffusion layer thickness but just by the thickness of the passivating oxide film.

Figure 12 exhibits typical impedance spectra on a Nyquist plot obtained from the pure aluminium rotating disc specimen at various rotation rates in 0.1 M NaOH + 0.5 M Na_2SO_4 solution. The impedance spectra consist of one capacitive semicircle in the high frequency region, one inductive semicircle in the intermediate frequency region, and one capacitive vertical line in the low-frequency region. Frers et al. [24] suggested an equivalent circuit for the native oxide-covered aluminium in which a high-frequency semicircle was attributed to the resistance of the passivating oxide film. The diameter of the high-frequency capacitive semicircle decreased with increasing rotation rate of the disc specimen, indicating the reduced resistance of the oxide film on the specimen.

The concentration of $Al(OH)_4^-$ ions at the oxide/solution interface is lowered with the increasing rotation rate of the specimen, by convection flow. The diminished $Al(OH)_4^-$ concentration will reduce the thickness of the oxide film by raising the dissolution rate of the oxide film according to Eq. (2). Therefore, the increase in the anodic current density and the decrease in the oxide film resistance with the rotation rate as shown in Fig. 11 and Fig. 12, respectively, are reasonably thought to arise from the decrease in the thickness of the passivating oxide film.

Based upon the experimental results, the repassivation kinetics of pure aluminium in aqueous solution can be split into three groups with the oxide dissolution rate, which strongly depends upon the pH of the solution. As

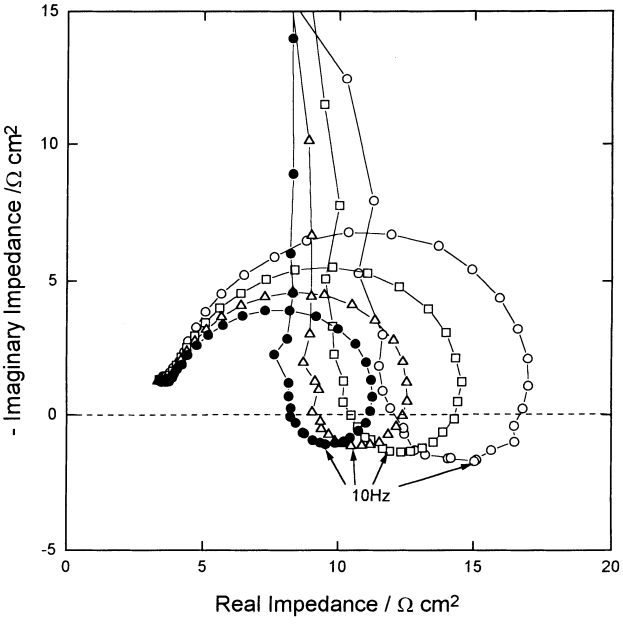

Fig. 12 Typical Nyquist plots obtained from the pure aluminium rotating disc specimen at an applied anodic potential of 0 V_{SCE} at various rotation rates in 0.5 M Na_2SO_4 + 0.1 M NaOH solution

the oxide dissolution rate is lowered, the single-staged behaviour in the anodic current transient clearly appears. This is the case of acidic [18], neutral [20] and weakly alkaline solutions below 0.001 M NaOH in 0.5 M Na_2SO_4. In contrast, when the oxide dissolution rate is intermediate (0.001 M and 0.1 M NaOH + 0.5 M Na_2SO_4), the anodic current transient shows two-staged behaviour which results from the attack by OH^- ions. Otherwise, in the case when the oxide dissolution rate is very high above 1 M NaOH in 0.5 M Na_2SO_4, three-staged behaviour is operative in the anodic current transient.

Conclusions

1. The amount of anodic polarisation at an open circuit markedly exceeded that of cathodic polarisation on the native oxide-covered surface of pure aluminium in aqueous alkaline solutions, suggesting that the corrosion rate is anodically controlled. By contrast, the anodic and cathodic polarisation occurred approximately to the same extent for the bare aluminium surface, indicating the mixed-controlled corrosion.

2. The repassivation rate of pure aluminium increased with increasing applied anodic potential and decreasing pH value in aqueous alkaline solutions.

3. Potentiostatic anodic current decay transients obtained from the moment just after interrupting the abrading action on pure aluminium specimens showed a constant repassivation rate in aqueous neutral and weakly alkaline solutions, but in concentrated alkaline solutions it was observed to be composed of the following three stages: a high repassivation rate in the initial stage due to the formation of a passivating oxide film on the bare surface; a zero value of the repassivation rate due to the dissolution of the oxide film in the second stage by the attack of OH^-; a high repassivation rate in the third stage due to a lowered dissolution rate of the oxide film by the increased concentration of the reaction product of $Al(OH)_4^-$ ions at the oxide/solution interface.

4. The anodic current density of pure aluminium was observed to be increased by the rotation rate of the specimen, which did not obey the Levich equation, suggesting that the lowered anodic current density is determined not by the diffusion layer thickness but by the thickness of the passivating oxide film.

References

1. Zaromb S (1962) J Electrochem Soc 109: 1125
2. Bocksite L, Trevethan D, Zaromb S (1963) J Electrochem Soc 110: 267
3. Tuck CDS, Hunter JA, Scamans GM (1987) J Electrochem Soc 134: 2970
4. Real S, Macdonald MU, Macdonald DD (1988) J Electrochem Soc 135: 2397
5. Albert IJ, Kulandainathan MA, Ganesan M, Kapali V (1989) J Appl Electrochem 19: 547
6. Macdonald DD, English C (1990) J Appl Electrochem 20: 405
7. Chu D, Savinel RF (1991) Electrochim Acta 36: 1631
8. Tabrizi MR, Lyon SB, Thompson GE, Ferguson JM (1991) Corros Sci 32: 733
9. Wilhelmsen W, Arnesen T, Hasvold O, Storkersen NJ (1991) Electrochim Acta 36: 79
10. Pyun S-I, Moon S-M, Ahn S-H, Kim S-S (1998) Corros Sci (in press)
11. Moon S-M, Pyun S-I (1997) Corros Sci 39: 399
12. Pearson HJ, Burstein GT, Newman RC (1981) J Electrochem Soc 128: 2297
13. Frankel GS, Rush BM, Jahnes CV, Farrell (1991) J Electrochem Soc 138: 643
14. Cinderey RJ, Burstein GT (1992) Corros Sci 33: 493
15. Pyun S-I, Hong M-H (1992) Electrochim Acta 37: 2437
16. Raetzer-Scheibe HJ, Tuck CDS (1994) Corros Sci 36: 941
17. Frankel GS, Jahnes CV, Brusic V, Davenport AJ (1995) J Electrochem Soc 142: 2290
18. Kim J-D, Pyun S-I (1995) Electrochim Acta 40: 1863
19. Kolman DG, Scully JR (1995) J Electrochem Soc 142: 2179
20. Pyun S-I, Lee E-J (1995) Electrochim Acta 40: 1963
21. Kim J-D, Pyun S-I (1996) Corros Sci 38: 1093
22. Kolman DG, Scully JR (1996) J Electrochem Soc 143: 1847
23. Barbosa M (1988) Corrosion 44: 149
24. Frers SE, Stefenel MM, Mayer C, Chierchie T (1990) J Appl Electrochem 20: 996